Density and size analysis of air separation process using MLA

M. Buchmann[1,2], T. Mütze[1], and F. Heinicke[3,*]

[1]*TU Bergakademie Freiberg, Institute of Mechanical Process Engineering and Mineral Processing, Agricolastr. 1, 09599 Freiberg, Germany; markus.buchmann@mvtat.tu-freiberg.de, thomas.muetze@mvtat.tu-freiberg.de*
[2]*Helmholtz-Zentrum Dresden-Rossendorf, Helmholtz Institute Freiberg for Resource Technology,13 Chemnitzer Straße 40, 09599 Freiberg, Germany; buchma78@hzdr.de*
[3]*Köppern Aufbereitungstechnik GmbH & Co. KG, Agricolastr. 24, 09599 Freiberg, Germany; f.heinicke@koeppern.de*
**Correspondence: f.heinicke@koeppern.de*

ABSTRACT

Dry air classification is a well-known technique used for decades in the cement industry to separate material in the size range of 0.01-1.0 mm. Additionally, in corresponding dry grinding circuits with effective machines such as High Pressure Grinding Rolls (HPGR), the energy consumption can be reduced compared to wet applications. These dry systems are not state of the art in minerals processing plants, but first prototypes have been installed and an increasing number of projects are starting to evaluate this option.

One challenge in this field is the mineral composition of ores, which have, by far, a higher variety in density and size than those of cement. High density particles such as iron- containing ones have higher settling rates than low density silica particles of the same size. The main question to answer in this paper is how to evaluate this effect, so a quantitative method using Mineral Liberation Analyses was developed to calculate two-dimensional partition curves. Additional statistical analyses allow for isolation and quantifying the interaction of density and size, enabling engineers to consider this effect for the sizing of process plants. The paper will present the method and selective results for a compounded ore of iron and silica.

Keywords: HPGR, air classification, partition curve, MLA

1. Introduction

The liberation size of ores decreased within the last decades and calls for a reduction of the cut size of classification systems [1]. This trend will go on for future reserves as well [2]. Dry screens are technical limited to perform this task. In addition, the availability and costs of water for spiral separators, wet screens or hydrocyclones is a major concern for plants, especially in dry mining zones (e. g. Chile, Peru, Mauretania or Australia) [3].

State of the art mining projects evaluate the application of HPGR technology versus SAG milling and other promising technologies [4,5]. In many cases, the HPGR enables power savings and reduces the load in the downstream ball mill. This has been successfully proven in test work and real industrial applications [6,7]. Fig. 1 represents a standard circuit with HPGR and screen in front of a ball mill.

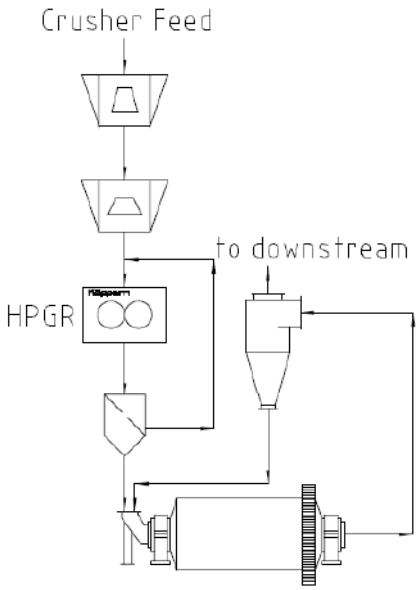

Fig. 1. State of the art HPGR flowsheet

According to the Bond theory [8] and its calculations for HPGR application [9] the transfer size from HPGR/screen circuit to ball mill is influencing the ball mill performance. Minimizing this transfer size reduces the total energy consumption for grinding due to the higher energy efficiency of the HPGR compared to the ball mill [10] and creates a higher circulating load within the HPGR grinding circuit. Additional physical effects like micro-cracks reduce the energy consumption of the ball mill even more [11,12].

The performance to separate material by screens decreases with lower transfer or cut size (see Fig. 2 [8]). This effect is due to smaller screen openings, reduced relative open cross-section and lower specific throughputs (volumetric limited), and can be countered by an increase of screen area. As mechanical restrictions and the high acceleration in modern screens are limiting the screen areas, the number of screens has to be increased at a certain point. An increase in number raises further questions in the flow sheet design, for example of how to distribute homogenously material to many screens.

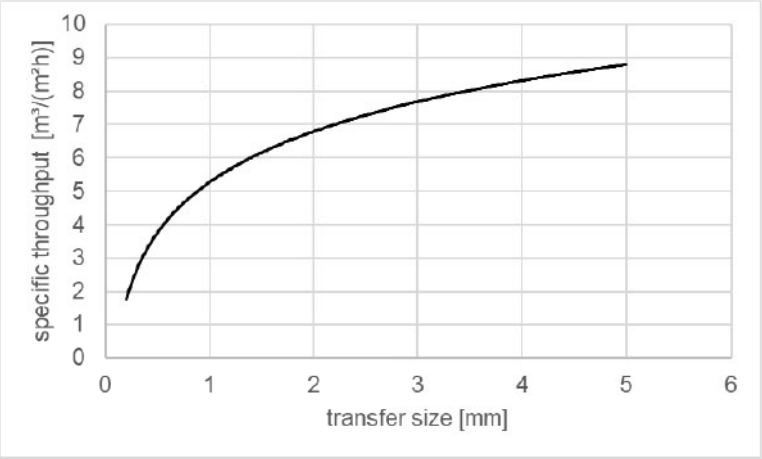

Fig. 2. Example of screen throughput depending on cut size (based on Schubert [13]).

The above mentioned challenges with respect to fine particles (i.e. in the lower µm-range) have already been addressed in the cement industry [14]. The highest energy savings were attained by finish grinding applications according to Fig. 3, where grinding is done in a HPGR and the low cut size is established by air classifiers. As the application of wet sieving is avoided, there is no requirement for high water consumptions in the process.

The cut size in air classifiers depends on the flow regime of the air and the particle properties including size and density [15]. Depending on the necessary degree of liberation, very fine cut sizes (eg. P80 of 0.03 mm) can be achieved for dynamic air classifiers by a low air throughput and high rotational speed of the classifier wheel [16,17]. Additionally, to a defined and narrow size distribution, two-stage air classifiers can produce medium-size product streams, which enable to use additional separators (e.g. magnetic separation devices). This opens up the potential for additional enrichment in the circuit [18].

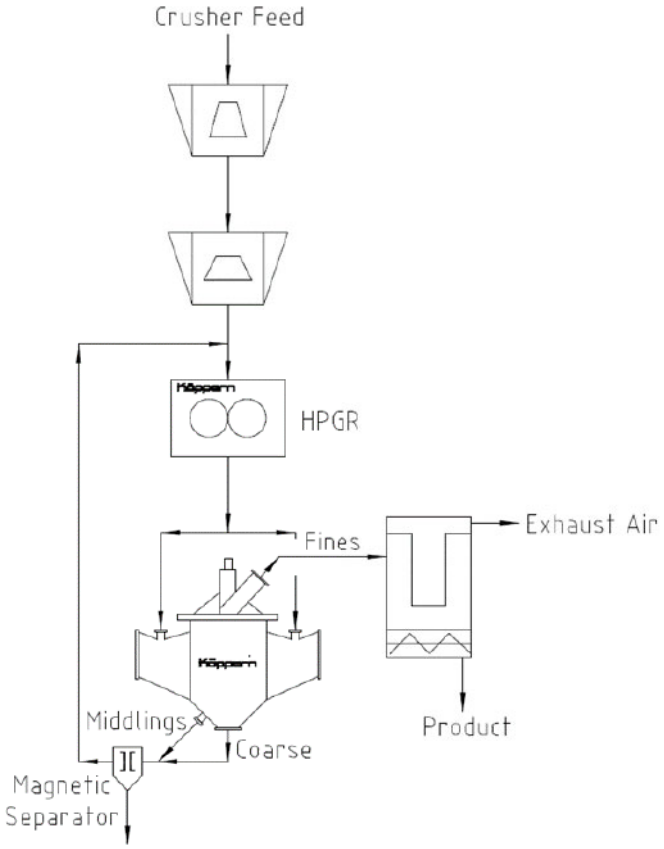

Fig. 3. Finish grinding circuit with HPGR and air classifier.

The enrichment with two-stage air classifiers can be positive when looking at the valuable mineral (e.g. iron content increases for downstream processing) or negative when looking at abrasive minerals (e.g. silica content increases in circulation loads). All those effects have to be evaluated, as the composition of minerals in ores is by far more complex than in cement applications.

One modern way to characterize mixtures of minerals is automated mineralogy or mineral liberation analysis (MLA). MLA generates particle based information on the basis of scanning electron microscopy (SEM) combined with an energy dispersive X-ray sensor (EDX) of particle cross sections [19]. In detail, the total area of the cross section and the partial areas of the individual mineral phases in the cross section are determined for each particle. Together with a database of the individual mineral densities, the respective particle density can be calculated as weighed average value. Those basic properties can be combined with other particle properties like characteristic sizes or susceptibility [20], which gives a matrix of particle information. Fig. 4 shows a schematic representation of the workflow from the particle sample to particle-based information via MLA. This or equivalent methods enable a multidimensional characterization of product and tailing streams as evaluation of e.g. separation processes as a function of different particle properties.

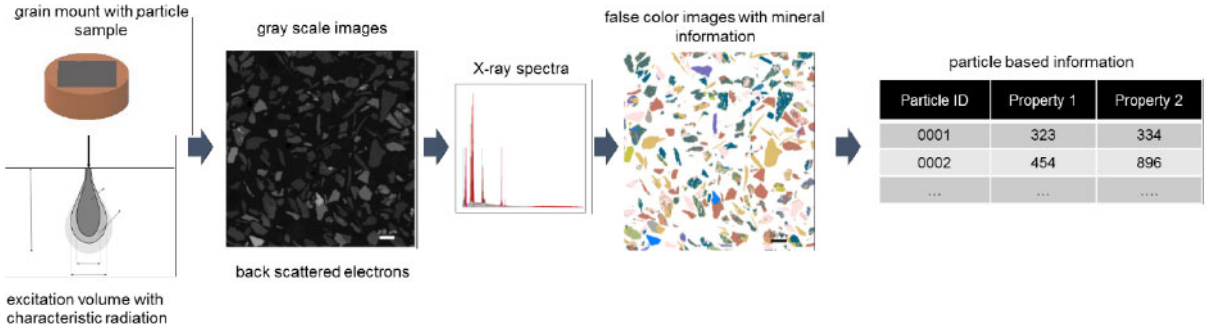

Fig. 4. Different steps of automated mineralogy (MLA) from particle sample to particle based information.

Since the particle information from MLA is based on a 2D evaluation some stereological bias might occur when transferring it to 3D parameters. The particle information matrix of MLA can be used to identify the most important properties for a certain separation process [21]. In the following sections the multidimensional characterization via MLA will be presented with the example of an air classification process of a certain iron oxide material.

2. Materials and Methods

The evaluation has been based on air classification test work, MLA analysis and special post processing.

2.1. Air Classification

A Turbo Classifier TC-15M manufactured by Nisshin Engineering was used for classification (Fig. 5). This classifier represents a dynamic counter current air classifier equipped with a classifier wheel, which utilizes a centrifugal field with forced eddy flow. The rotational speed of the wheel, the airflow rate and the feeding rate can be adjusted in order to get cut sizes between 1 and 100 µm. The tests shown here were conducted at an air flow rate of 2.2 m^3/min at various rotor speeds in order to get theoretical cut sizes between 35 and 90 µm. These theoretical cut sizes were calculated according to the classifier calibration algorithm, which considers the average particle density. In turn, the density was determined to 4.0 g/cm^3 measured by Helium pycnometry (AccuPyc II 1340, Fa. Micromeritics).

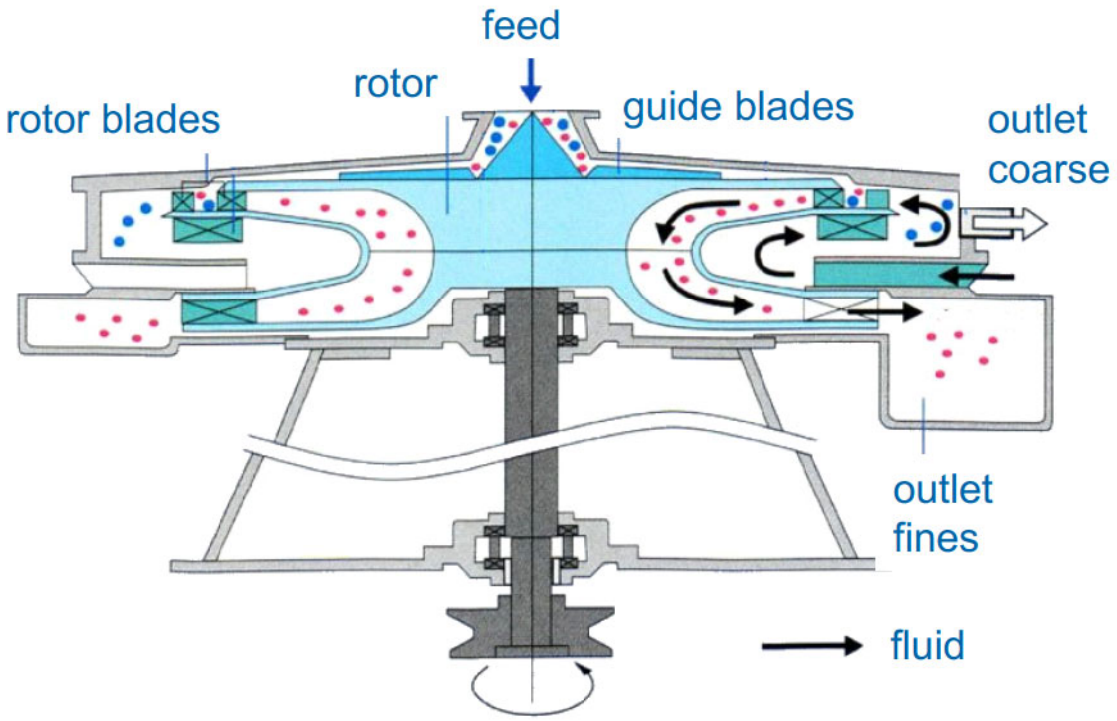

Fig. 5. Schematic drawing of the Turbo Classifier TC-15M (Nisshin Engineering).

The applied feed material represents an iron ore with a particle size distribution < 250 µm. According to MLA, the main minerals of this material are Fe-oxides (65 wt.-%), silicates (30 wt.-%) and some other minerals with minor contents (e.g. carbonates). Each test and measurement was performed with representative samples of the feed material (700 to 750 g) or classification products (130 to 630 g). Conventional riffle splitters or rotational splitters were used to produce analytical samples by standard procedures.

2.2. Evaluation of MLA Results

Polished epoxy blocks of the samples from the air classification tests with a diameter of 30 mm were prepared. The sample material was mixed with graphite for a better separation of the particles and then embedded in epoxy resin. The resulting block was cut in slices, turned by 90° and embedded in epoxy again. Thus, for further investigations on the sample surfaces via Mineral Liberation Analysis (MLA) any separation effects due to gravitational settling of the particles were minimized. MLA is an automated SEM-based image analysis method, comprising a scanning electron microscope FEI Quanta 650F equipped with two Bruker Quantax X-Flash 5030 energy-dispersive X-ray spectrometers and the MLA 3.1.4 software suite for automated data acquisition. All samples were analyzed using the grain X-ray mapping (GXMAP) mode [19]. Standard spectra were collected for all relevant minerals [22].

The discrete information coming from MLA on a particle level can be transferred to a continuous representation by the method of kernel density estimation [23,24]. In Fig. 6a the particles of the feed material for the air classification tests are shown regarding their property combination of size x_P and

density ρ_P. Each dot represents one particle found in exactly this MLA sample. Every MLA measurement can be represented by a likewise manner. The kernel density estimation generates a Gaussian kernel around each data point (particle) and a hull curve for all data points (particles) by overlapping these kernels. This concept is visualized in one dimension (x) in Fig. 6b. By weighting the kernels with the respective mass of each particle, the mass distribution is achieved as a function of two characteristic particle properties (particle size xp and particle density , see Fig. 6c). The equivalent circle diameter (ECD) is used as size parameter here, but any other 2D size parameter could be utilized. The following considerations are all based on particle size (x_P) and particle density (ρ_P).

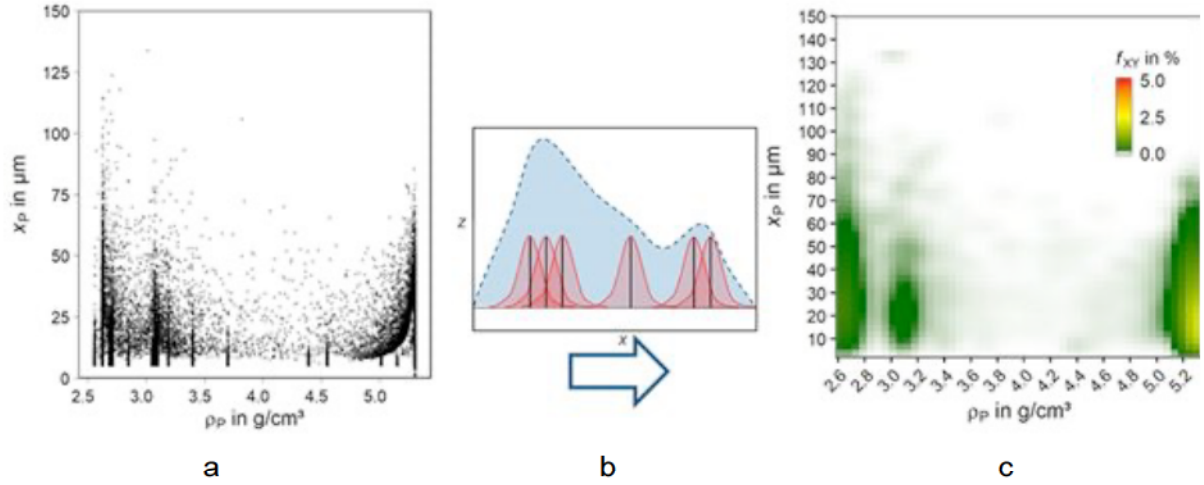

Fig. 6. Transferring the discontinuous particle based data from MLA (a) to a continuous density distribution of the particle mass (c) via kernel density estimation (b).

The resolution of the multidimensional representation is based on a kernel density estimation, which produces a continuous distribution. Nevertheless, a certain resolution has to be chosen for the visualization of the distribution like in fig. 6c or the following. The presented resolution of 50x50 pixel is sufficient to identify certain material specific effects in the investigated example. The increase of calculation time which is necessary for a higher resolution was not reasonable for the actual example [23,25].

The mass distribution of the applied feed material (mineral composition see section 2.1) is visualized with the help of a color scale. The whole area sums up to 100 % of the particle mass and covers a size range from 2 to 150 µm and a range of particle densities from 2.5 to 5.5 g/cm³. Within these property ranges are preferred property combinations where most of the particles and therefore the mass of the feed material accumulates. Two main areas can be identified: a region at approx. 5.2 g/cm³ associated to Fe-oxide and a region at 2.6 – 3.2 g/cm³ mostly associated to silicates. These two areas represent more or less liberated particles where only one of these mineral groups is present. The intermediate densities between these two regions represent particles with more or less intergrown mineral phases.

Separation processes and especially classification processes are often evaluated by partition curves (or Tromp curves). For particles of defined properties (e.g. a certain size) the partition curve describes the probability to be transferred to a certain product (e.g. the coarse product of a classification process). Originally, these curves are based on one major property (e. g. particle size for classification processes) that influences most significantly the separation result. In this case, the partition curve is calculated and visualized as a function of this (single) major property.

As already stated most separation processes are not only influenced by a single material property, but rather by a combination of different properties. With the kernel density estimation an extension of the one-dimensional partition curve to a two-dimensional partition map is possible. In Fig. 7 the expansion from such a 1D curve (based on one particle property ξ_1) to a 2D map (based on two particle properties ξ_1 and ξ_2) is depicted. For visualization, the probability to be transferred is shown via colour scale in the 2D map.

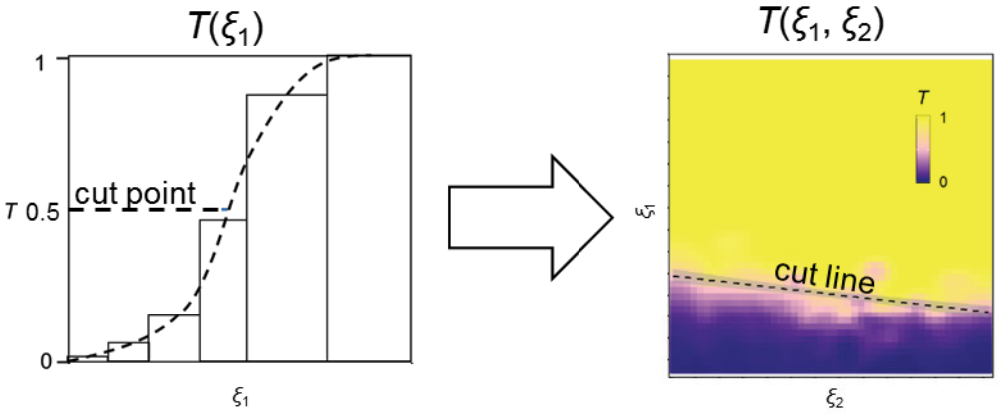

Fig. 7. Transition of a one-dimensional partition curve (left) to a partition map (right) based on two particle properties

The cut line represents a function of the particle properties ξ_1 and ξ_2. In analogy to the cut point in the 1D case it represents a regression line for the value of T in a range of 45 % to 55 %. From this perspective, a cut point is an average separation result regarding particle property ξ_1 depending on the process as well as the composition of the feed material regarding particle property ξ_2. Through partition maps, a direct assessment of the separation process as function of two or even more material properties is possible. The process result can be evaluated for multiple individual materials in the mix of the feed (in our case: particles of different densities and therefore also composition). The maps allow also to estimate the magnitude of influences from different material properties on the separation result like particle density or particle shape (not shown) in the case of air classification.

3. Results and discussion

The classification tests are analyzed with the approach presented in section 2.2. The main components of the material are silicates and Fe-oxides. In addition, the distribution of these two mineral

groups can be illustrated if the kernel density estimation is used only for the mineral mass of one specific mineral phase. In Fig. 8 this is done for the silicates and the Fe-oxides of the feed material. The mineral mass distribution for each depicted mineral group sums up to 100 %.

For the Fe-oxides, the majority of the mineral mass is in the range of the density value 5.2 g/cm³ and below a particle size of 100 µm. The particles in this range indicate high liberation of Fe-oxides as the particle density meets more or less the density of Fe-oxides (hematite and magnetite). Nevertheless, the mineral mass distribution of Fe-oxides also indicates Fe-oxides in lower density ranges. This corresponds to the mass of Fe-oxides more or less intergrown with other minerals.

A comparable situation appears for the silicates, which are mainly (83 %) quartz and actinolite. In comparison to the Fe-oxides, the silicates appear to some extent above 100 µm but with a majority below 100 µm. The majority of the mass of the silicates appears in a rather low density range (<3.6 g/cm³), but there is also an amount of silicates containing particles at higher density values due to a low amount of minerals like enstatite (density up to 3.9 g/cm³) or silicate phase which are intergrown with Fe-oxides.

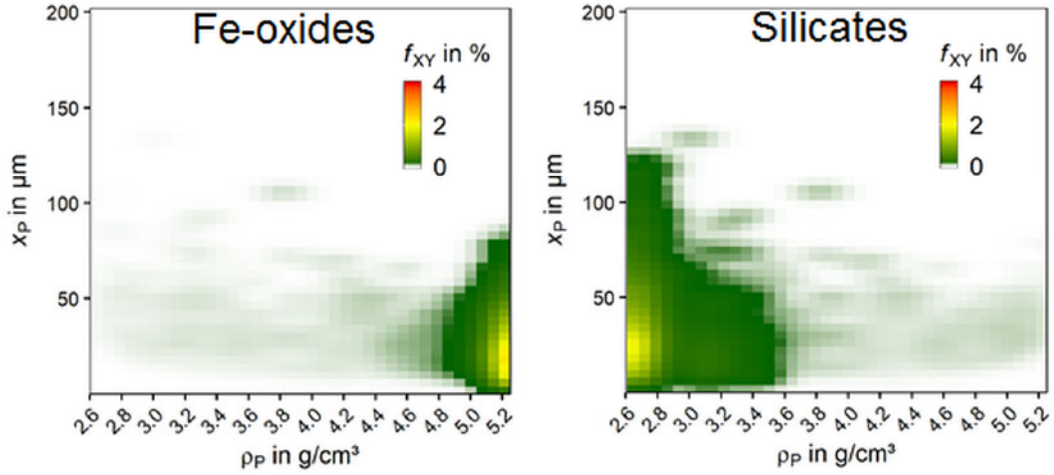

Fig. 8. Mineral mass distribution for Fe-oxides and silicate as a function of particle size and particle density (feed material)

In Fig. 9 the partition maps (*T*-maps) of the classification tests of the presented feed material with three different cut sizes (theoretical cut size: a: 35 µm, b: 60 µm and c: 90 µm) are shown. For the assessment of the classification process, the partition map is used as presented in chapter 2.2. In Fig. 9 the probability of a particle to be transported to the coarse product is visualized with the help of a continuous color scales for the values between 0 % (purple) and 100 % (yellow). Two main areas are visible in three tests in Fig. 9: The yellow area shows an enrichment of the respective particle with these property combinations in the coarse product. The purple area is associated to low particle sizes and represents mainly a depletion of the respective property combinations in the coarse product. This is expected since small particles are mainly to be transferred to the fine product in a classification process. Between these two main areas a transition zone exists (with 0 % < T < 100 %) for which no clear

assignment is possible whether the particle with this property combination will go to the coarse or the fine product. To increase the separation efficiency of the classification process, this transition zone needs to be minimized via process parameter adjustment as part of the typical process optimization.

The partition maps indicate the much stronger influence of the particle size on the classification process compared to particle density. Nevertheless, there is an influence of the particle density on the separation process visible. The cut size is shifted to lower values with increasing particle density. This effect is less pronounced in case a (35 µm cut size) and increases with increasing cut size. Nevertheless, the cut size is a function of the particle density and associated with the respective mineral group. For the heavy minerals (Fe-oxides in the range of 5 g/cm³) smaller particle are transferred to the coarse product compared to the lighter silicates.

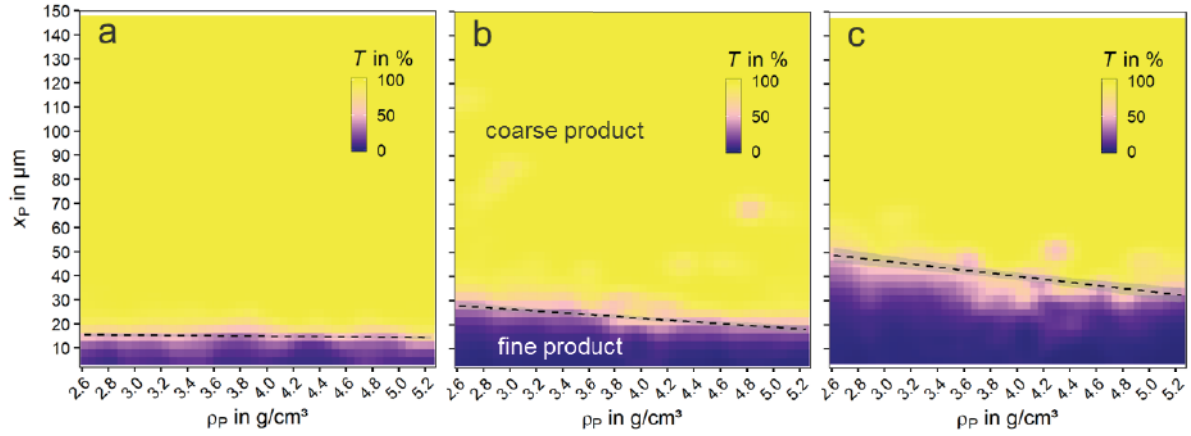

Fig. 9. *T*-maps of the investigated classification tests for three different cut sizes as function of particle size and particle density (theoretical cut sizes 35 µm (a), 60 µm (b) and 90 µm (c))

Based on the theory of partition curves as a function of one characteristic property there are ideal cases of such partition maps. These ideal cases are depicted in Fig. 10. The cases (a) and (b) describe a behavior, where the separation process is only depending on one of the investigated particle properties. Case (c) represents an example of a separation process depending on both properties. In (d) an ideal splitting is described with a constant value of *T* for the whole area. The ideal splitting equals two products with the same composition as the feed material regarding the property combination of *X* and *Y*.

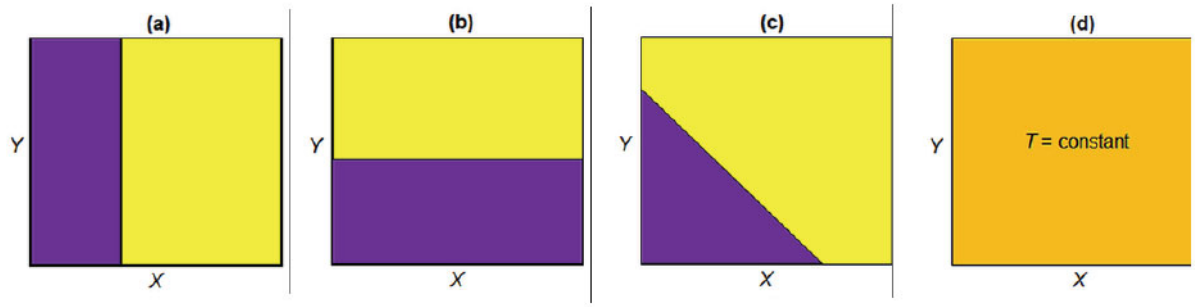

Fig. 10. Possible cases of partition maps; (a) and (b): one of the investigated particle properties only influences the separation process; (c) both particle properties influence the separation process, (d) ideal splitting

Ideal cases show a behavior where the transition from 0 % to 100 % is represented by a step function. In reality (Fig. 10) there will be a transition zone between these two areas with values between 0 and 100 %. The extent of this transition zone defines the separation efficiency, i.e. the quality of the separation process. To minimize this zone will be the goal of process optimization and is closely related to the individual separation device. Another approach could be to minimize the amount of material associated to the corresponding combinations of particle properties by optimizing upstream processes like the grinding in an HPGR.

5. Conclusions and outlook

The application of SEM-based particle analysis (i.e. MLA) and the related post processing enables to evaluate the effect of the different particle properties on air classification. In the present case study, the combined effect of particle size and particle density was investigated. With the proposed approach, combined property effects are assessable to get a better understanding of the investigated process. Various other particle properties are accessible via MLA. Therefore, a huge variety of processes can be analyzed with the presented method as shown in [25] and complete flow sheets can be assessed to characterize the different processes in a multidimensional approach. Further, the applied characterization method via kernel density estimation and multidimensional partition maps is not limited to data from MLA, but is applicable to each particle-based data. The general approach to extend the influence of the size in separation processes can therefore deliver additional information to consider physical effects in design and optimization of processing plants.

Author Contributions: Conceptualization, F.H. and T.M.; methodology, M.B.; validation, M.B., F.H. and T.M.; investigation, T.M.; resources, F.H.; data curation, M.B.; original draft preparation, M.B., F.H. and T.M.; writing—review and editing, T.M., F.H. and M.B.; visualization, M.B.; supervision, F.H. and T.M.; project administration, T.M.; funding acquisition, F.H. and T.M. All authors have read and agreed to the published version of the manuscript.

Acknowledgments

The authors would like to thank Köppern for supporting this research project.

Conflicts of Interest

"The authors declare no conflict of interest."

References

1. Sousa, R.; Simons, B.; Bru, K.; de Sousa, A.B.; Rollinson, G.; Andersen, J.; Martin, M.; Machado Leite, M. Use of mineral liberation quantitative data to assess separation efficiency in mineral processing – Some case studies. *Minerals Engineering* **2018**, *127*, 134-142, doi:10.1016/j.mineng.2018.08.004.

2. Jones, H.; Boger, D.V. Sustainability and Waste Management in the Resource Industries. *Industrial & Engineering Chemistry Research* **2012**, *51*, 10057-10065, doi:10.1021/ie202963z.

3. Ihle, C.F.; Kracht, W. The relevance of water recirculation in large scale mineral processing plants with a remote water supply. *Journal of Cleaner Production* **2018**, *177*, 34-51, doi:10.1016/j.jclepro.2017.12.219.

4. Costello, B.; Brown, J. A tabletop cost estimate review of several large HPGR projects. In Proceedings of Proceedings of SAG (Vancouver); pp. 1-24.

5. Baawuah, E.; Kelsey, C.; Addai-Mensah, J.; Skinner, W. Economic and Socio-Environmental Benefits of Dry Beneficiation of Magnetite Ores. *Minerals* **2020**, *10*, 955, doi:10.3390/min10110955.

6. Gardula, A. First year operation of HPGR at Tropicana Gold Mine. In Proceedings of Proceeding of SAG (Vancouver).

7. Vanderbeek, J.L.; Gunson, A.J. Cerro Verde 240.000 t/d concentrator expansion. In Proceedings of Proceedings of SAG (Vancouver).

8. Bond, F.C. The third theory of comminution. In Proceedings of Mining Engineering; pp. 484-494.

9. Heinicke, F.; Hubert, A. Improvement of CIS standard iron ore circuit by HPGR. In Proceedings of Proceedings of SAG (Vancouver); pp. 1-10.

10. van der Meer, F.P.; Schnabel, H.G. The effect of roller press grinding on ball mill energy. In Proceedings of Erzmetall; pp. 554-561.

11. Michaelis, H. Real and potential metallurgical benefits of HPGR in Hard Rock Ore Processing. In Proceedings of Proceedings of Randol Conference; pp. 1-9.

12. Bru, K.; Sousa, R.; Leite, M.M.; Broadbent, C.; Stuart, G.; Pashkevich, D.; Martin, M.; Kern, M.; Parvaz, D.B. Pilot-scale investigation of two Electric Pulse Fragmentation (EPF) approaches for the mineral processing of a low-grade cassiterite schist ore. *Minerals Engineering* **2020**, *150*, 106270, doi:10.1016/j.mineng.2020.106270.

13. Schubert, H. *Handbuch der Mechanischen Verfahrenstechnik*; Weinheim: Wiley VCH: 2003.

14. Aydoğan, N.A.; Ergün, L.; Benzer, H. High pressure grinding rolls (HPGR) applications in the cement industry. *Minerals Engineering* **2006**, *19*, 130-139, doi:10.1016/j.mineng.2005.08.011.

15. Shapiro, M.; Galperin, V. Air classification of solid particles: a review. *Chemical Engineering and Processing: Process Intensification* **2005**, *44*, 279-285, doi:10.1016/j.cep.2004.02.022.

16. Altun, O.; Toprak, A.; Benzer, H.; Darilmaz, O. Multi component modelling of an air classifier. *Minerals Engineering* **2016**, *93*, 50-56, doi:10.1016/j.mineng.2016.04.014.

17. Guo, L.; Liu, J.; Liu, S.; Wang, J. Velocity measurements and flow field characteristic analyses in a turbo air classifier. *Powder Technology* **2007**, *178*, 10-16, doi:10.1016/j.powtec.2007.03.040.

18. van der Meer, F.P. Feasibility of dry High Pressure Grinding and Classification. In Proceedings of Proceedings of SAG (Vancouver); pp. 1-18.

19. Fandrich, R.; Gu, Y.; Burrows, D.; Moeller, K. Modern SEM-based mineral liberation analysis. *International Journal of Mineral Processing* **2007**, *84*, 310-320, doi:10.1016/j.minpro.2006.07.018.

20. Buchmann, M.; Schach, E.; Leißner, T.; Tolosana-Delgado, R.; Kern, M.; Krupko, N.; Rudolph, M.; Peuker, U. Density and susceptibility: Geometallurgical characterization of a cassiterite-bearing complex skarn ore from the Ore Mountains, Germany. In Proceedings of 29th International Mineral Processing Congress, Moscow; pp. 4042-4050.

21. Buchmann, M.; Schach, E.; Tolosana-Delgado, R.; Leißner, T.; Astoveza, J.; Kern, M.; Möckel, R.; Ebert, D.; Rudolph, M.; van den Boogaart, G., et al. Evaluation of Magnetic Separation Efficiency on a Cassiterite-Bearing Skarn Ore by Means of Integrative SEM-Based Image and XRF–XRD Data Analysis. *Minerals* **2018**, *8*, 390, doi:10.3390/min8090390.

22. Bachmann, K.; Osbahr, I.; Tolosana-Delgado, R.; Chetty, D.; Gutzmer, J. Variation in Platinum Group Mineral and Base Metal Sulfide Assemblages in the Lower Group Chromitites of the Western Bushveld Complex, South Africa. *The Canadian Mineralogist* **2018**, *56*, 723-743, doi:10.3749/canmin.1700094.

23. Schach, E.; Buchmann, M.; Tolosana-Delgado, R.; Leißner, T.; Kern, M.; van den Boogaart, G.; Rudolph, M.; Peuker, U. Multidimensional characterization of separation processes – Part 1: Introducing kernel methods and entropy in the context of mineral processing using SEM-based image analysis. *Minerals Engineering* **2019**, *137*, 78-86, doi:10.1016/j.mineng.2019.03.026.

24. Kupka, N.; Tolosana-Delgado, R.; Schach, E.; Bachmann, K.; Heinig, T.; Rudolph, M. R as an environment for data mining of process mineralogy data: A case study of an industrial rougher flotation bank. *Minerals Engineering* **2020**, *146*, 106111, doi:10.1016/j.mineng.2019.106111.

25. Buchmann, M.; Schach, E.; Leißner, T.; Kern, M.; Mütze, T.; Rudolph, M.; Peuker, U.A.; Tolosana-Delgado, R. Multidimensional characterization of separation processes – Part 2: Comparability of separation efficiency. *Minerals Engineering* **2020**, *150*, 106284, doi:https://doi.org/10.1016/j.mineng.2020.106284.